Low Temperature Physics/Fizika Nizkikh Temperatur, 2019, v. 45, No. 10, pp. 1249–1256

Superconductivity and weak anti-localization in GaSb whiskers under strain

N. Liakh-Kaguy, A. Druzhinin, I. Ostrovskii, and Yu. Khoverko

Lviv Polytechnic National University, S. Bandera Str., 12, Lviv 79013, Ukraine
E-mail: druzh@polynet.lviv.ua

Received February 20, 2019, revised April 3, 2019, published online August 27, 2019

Strain influence on the behavior of temperature dependences of resistance was studied in the *n*-type conductivity GaSb whiskers with tellurium concentration $1.7 \cdot 10^{18}$ cm^{-3}. Analyzing these dependences in the temperature range 4.2–30 K strain inducted metal–insulator transition and partial superconductivity were found in the whiskers. The transverse and longitudinal magnetoresistances for unstrained and strained GaSb whiskers were also studied in ranges of magnetic field 0–3 T and temperature 1.5–60 K. The effects, such as a superconductivity and weak anti-localization were observed for unstrained and strained samples. The upper critical zero magnetic fields for superconductivity suppression were obtained in the whiskers. Strain was shown to decrease the superconductivity in GaSb samples. The strain induced splitting of degenerate level on two components with opposite and parallel spins was found in the *n*-type conductivity GaSb whiskers due to weak localization and anti-localization effects, respectively.

Keywords: GaSb whiskers, strain influence, transverse and longitudinal magnetoresistance, superconductivity, weak localization and anti-localization.

1. Introduction

Topological insulators are new type of the quantum materials defined by prevalence of a gap in energy spectrum. They also characterized by symmetrically protected surface states within a volumetric gap [1,2]. Various interesting behavior of the topological insulators, especially in the protected surface states, was studied due to transport mechanisms [3–7].

Spin-momentums blocked surface states always observe weak anti-localization (WAL) due to strong spin-orbit interaction [8–9]. Bulk states of 3D topological insulators are not perfectly isolated even at extremely low temperatures, as a result they can affect the transport mechanisms. In contrast to the symmetric protected surface states, the bulk topological states with intense spin-orbit interaction (SOI) could cause to WAL or localization depending on conditions of experimental studies [10,11]. Crossover from WAL to weak localization (WL) of bulk states was shown in the longitudinal magnetoresistance up to 50 T [10]. The magnetoresistance anisotropy with the magnetic field orientation means the intrinsic SOI in Bi_2Se_3 films. This crossover in quantum interference effect of bulk states open up prospects for the creation of nano-scale devices due to the studies of three-dimensional topological insulators [10]. The authors of the work [11] proved that the temperature decreasing leads to WL suppresses the conductivity, but WAL increases the conductivity at extremely low temperatures. The crossover from WAL to WL was also predicted and experimentally confirmed due to massless Dirac fermions (surface states of the topological insulator) gain its mass.

Quantum interference effect could be destroyed by the magnetic field that gives to increasing cusp-like positive and negative magnetoconductivity corresponding to WL and WAL, respectively [11–14]. Therefore, topologically protected surface states could not be localized in the topological insulators that is advantage over metals [1,15].

Measurements of the device differential gain in GaAsSb quantum wells under compressive strain show improvement of the laser threshold [16]. The biaxial compressive strain leads to increasing of hole mobility caused by a reduction their effective mass due to modulation of valence bands in devices on base GaSb structures [17]. The influence of the strain created due to the difference between crystalline lattices in heterostructures on the above-described effects is given in works [18,19]. Strained GaSb whiskers were used as pressure sensors [20]. The temperature dependent magnetotransport measurements were shown in the InAs/GaSb quantum wells. The WAL that dominant spin-orbit relax-

ation mechanism for low-mobility heterostructures is Elliott–Yafet, but not Dyakonov–Perel in form of Rashba or Dresselhaus SOI [19].

The magnetic properties of the InSb whiskers were studied at low temperatures and magnetic field 0–14 T [21]. The superconductivity (SC) has been revealed on the magnetoresistance dependences at temperature lower than 4.2 K in our previous works for the *n*-type conductivity GaSb whiskers doping with tellurium [22]. This effect has also revealed and investigated at low temperatures in many structures based on the bismuth [23,24]. The studies of the magnetoresistance dependences of doped Bi_2Se_3 whiskers give us the opportunity to reveal the SC and Kondo effect in weak magnetic fields [24]. We already have established the week anti-localization model of the *n*-type conductivity GaSb whiskers due to the strong spin–orbit interaction in work [22]. Crossover of the quantum interference effect from WAL to WL was shown in the GaSb whiskers [25]. Interesting strain induced effect of InSb whiskers as Berry phase was studied in our previous work [26]. We also predicted to found the interesting quantum interference effects in the strained GaSb whiskers.

The aim of the article is studies of strain influence on the *n*-type conductivity GaSb whisker longitudinal and transverse magnetoresistance at weak magnetic fields and low temperatures 1.5–60 K. SC and WAL were revealed in the studied samples under strain.

2. Experimental procedure

Object of our studies was *n*-type conductivity GaSb whiskers obtained by method of chemical transport reactions. Investigated whiskers were doped with Te during their growth. GaSb whiskers were selected with the diameter 20–30 μm and the length 2–3 mm. Au microwire with diameter of 10 μm was used to create electrical contact to the samples that form an eutectic with crystal under the pulsed welding. The pulse welding took place at the sample heating to temperature of about 500 K with the next annealing to avoid the local deformations in contact regions. That technique allows measuring whisker resistance using the four contact scheme along the microcrystal (the longitudinal resistance). The additional contact was made to study the galvanomagnetic properties in GaSb samples. The linear *I–V* characteristics indicated the ohmic contact, which resistance did not exceed 0.1% of the whisker resistance.

GaSb whiskers were strained due to mounting of the microcrystal on substrates with a thermal expansion coefficient different from the GaSb material. Similar technique with thermal strain using was shown in *n*-type conductivity InSb whiskers by authors of work [26]. Copper substrate was used to create a uniaxial compressive strain ($\varepsilon = -3.8 \cdot 10^{-3}$ rel. units) at temperature 4.2 K. The thermal compressive strain with a direction <111> was calculated in GaSb samples in the temperature range 4.2–60 K.

Low-temperature magnetoresistance of GaSb whiskers was investigated in the temperature range 1.5–60 K. For the studies samples were placed in helium cryostat where crystals were cooled to the temperatures 1.5–4.2 K. Temperature was measured by thermocouple of Cu–CuFe. The magnetic field effect on properties of GaSb whiskers was studied due to use a Bitter magnet with induction up to 3 T and field time scanning of 1.75 T/min at temperature 1.5–60 K. The stabilized electric current through the samples was created using current source Keithley 224 with current range 1–10 μA depending on the whisker resistance. Such currents are known to lead to overheating the samples at very low temperatures [27]. In our experiment we have checked *I–V* characteristics of the samples in order to determine the critic current leading to curve saturation, which indicates in overheating the sample. A deviation from line of *I–V* characteristics takes place at current exceeding 10 mA. Thus, very small current (a few μA) were used in the experiment that hardly results in overheating the charge carriers in the whiskers. To avoid the effect of parasitic thermo-emf or contact potential difference the altering current (ac) with frequency of 20 Hz was also passed through the certain samples. The same results were obtained in both ac and dc measurements indicating in the absence of thermo-emf or contact potential difference.

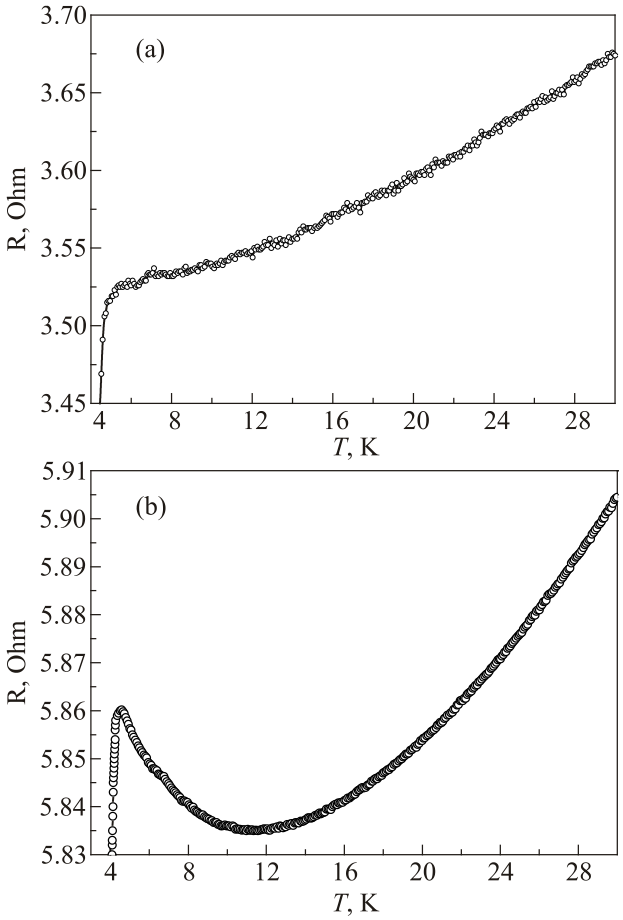

Fig. 1. Temperature dependences of resistance in unstrained (a) and strained (b) GaSb samples.

We have used two geometries of experiment depending on the direction of applied magnetic field. When a magnetic field is applied parallel/perpendicular to current direction in the samples, the longitudinal/transverse magnetoresistance was determined.

3. Experimental results

Temperature dependences of GaSb whiskers resistance in temperature range 4–30 K were plotted on Figs. 1(a), (b) for unstrained and strained samples, respectively. As you can see from the figure, temperature dependence of the resistance for unstrained whiskers is typical for metallic samples, however, at temperature 4.2 K a straight drop of the resistance occurs, which is probably connected with partial SC of the whiskers. It is obvious that strain influences the whiskers resistance substantially. Firstly, a large minimum of the resistance appears at temperature of about 10 K. Secondly, a partial transition to superconductive state (straight drop of the whisker resistance takes place at temperature of about 4.2 K). A large minimum of the resistance is likely resulted from the strain inducted metal–insulator transition (MIT) to insulator phase at temperature below 11 K. To explain the above effects one can consider the whiskers magnetoresistance.

Transverse and longitudinal magnetoresistances for unstrained and strained GaSb whiskers were shown on Figs. 2(a), (b) and Figs. 3(a), (b), respectively. As seen from Fig. 2(a), the typical quadratic field dependences of the whisker transverse magnetoresistance are observed in temperature range over 4.2 K. At temperatures below 4.2 K a straight rise of the whisker magnetoresistance takes place in low magnetic fields (see Fig. 2(a)). An application of strain changes drastically a behavior of the whisker magnetoresistance — it becomes negative at small temperatures in all range of measured temperatures.

The similar behavior of the GaSb whisker magnetoresistance is observed when a magnetic field is applied parallel to current direction in the samples, i.e., for longitudinal magnetoresistance. For unstrained samples anomal magnetoresistance occurs only at temperatures 4.2 K and lower temperatures (see Fig. 3(a)). For strained samples a complex behavior of the whisker magnetoresistance is observed:

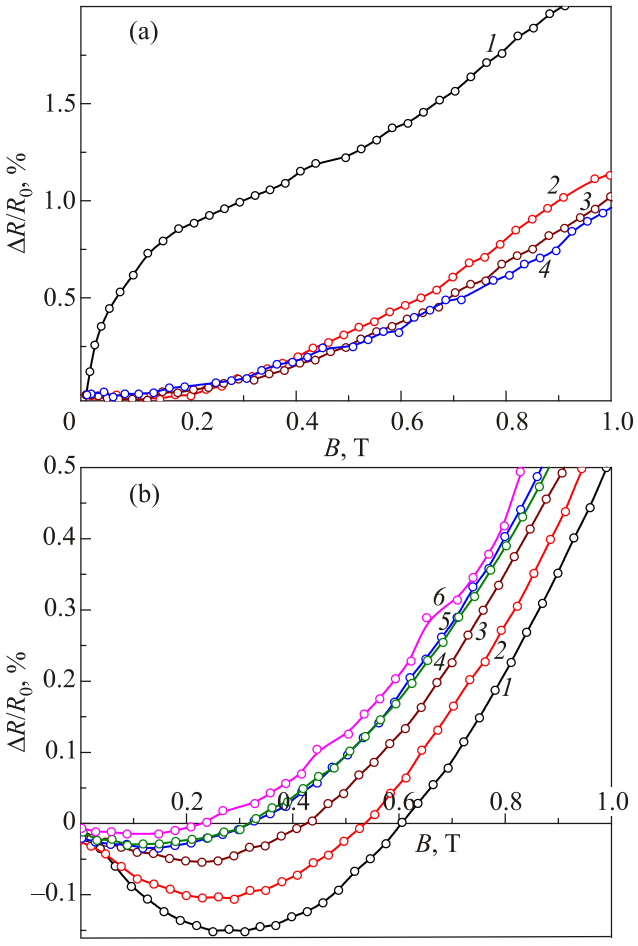

Fig. 2. (Color online) Transverse magnetoresistance of GaSb whiskers for unstrained (a) and strained (b) samples at temperature, K: 4.2 (*1*), 13 (*2*), 29 (*3*), 40 (*4*), 50 (*5*), 60 (*6*). $\Delta R = R_B - R_0$, where R_B and R_0 are the whisker resistance at non-zero and zero magnetic field induction, respectively.

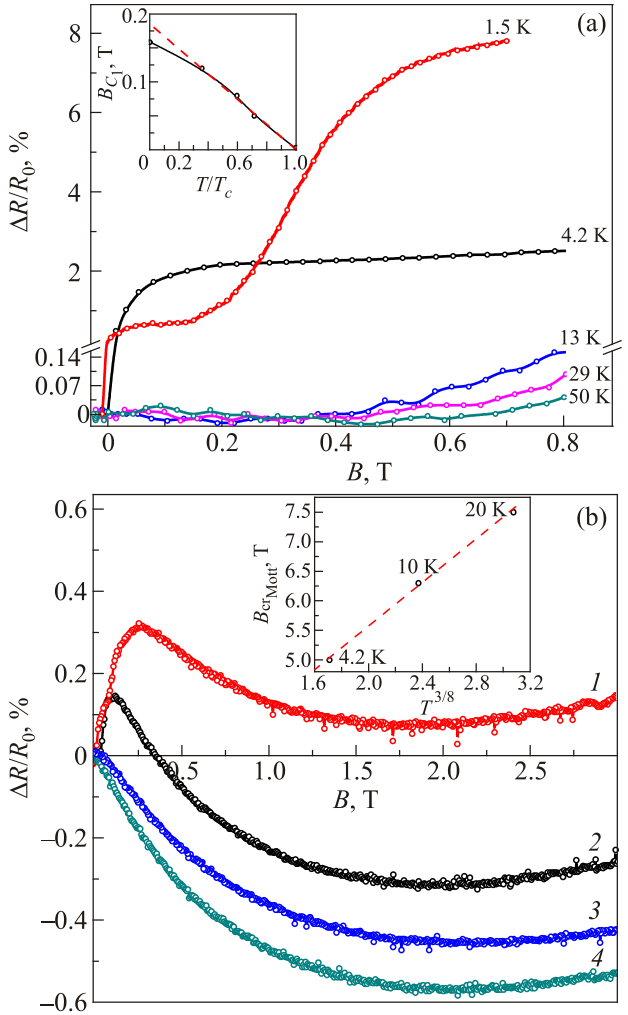

Fig. 3. (Color online) Longitudinal magnetoresistance of GaSb whiskers at various temperatures for unstrained (a) and strained (b) samples. Inserts: zero critical magnetic field (a); B_{cr} versus $T^{3/8}$ (b).

at temperatures below 10 K magnetoresistance rises occur at low magnetic fields, while at higher temperatures a transition to negative magnetoresistance on the field dependences of magnetoresistance is observed (see Fig. 3(b)).

4. Discussion

In order to determine an influence of strain on the whisker parameters one can compare the behavior of magnetoresistance in unstrained and strained samples.

4.1. *Unstrained* GaSb *whisker magnetoresistance*

Field dependence of GaSb whisker longitudinal magnetoresistance below 4.2 K was interpreted as transition in SC state [22]. An analysis of upper critical magnetic fields gives zero temperature critical magnetic field 1.1 T for SC suppression. On the other hand, the upper critical zero magnetic field 0.08 T was determined from the data of the whisker magnetic susceptibility, which is in order magnitude lower than the above one [22]. A big discrepancy between the data indicates that the main contribution of the magnetoresistance jump in magnetic fields with intensity 0.1–0.75 T is not connected with SC. The magnetoresistance behavior can be connected with two possible reasons: weak localization and electron-electron interaction (EEI) or the co-existing of the above effects [28]. The effect of WL takes place in diffuse regime when $k_B T\tau/h < 1$, while in transition and ballistic regime when $k_B T\tau/h > 1$ EEI effect prevails [28]. On the other hand, the WL effect occurs at weak magnetic fields, while EEI effect is observed at strong magnetic fields [29]. In our study we consider the effect at weak magnetic fields that indicates the WL effect predominance in the whiskers. Moreover, very small current (a few μA) were used in our experiment that hardly results in overheating the charge carriers in the whiskers. Therefore, the most probable reason of the effect is WAL of charge carriers. Nevertheless, we have observed one more magnetoresistance jump at low magnetic fields (see Fig. 3(a)). One can obtain the upper critical zero magnetic fields from the magnetoresistance jumps at various temperatures. The results are provided on the insert of Fig. 3(a) and give $B_{cr} \sim 0.16$ T. The value is comparable with that obtained from magnetoresistance investigations, which indicates in SC transition of GaSb whiskers at low magnetic fields.

Therefore, at low temperatures 1.5–4.2 K two effects could coexist in GaSb whiskers — SC and WAL. Magnetic field suppressed the above effect. Suppression of SC takes place at $B_{cr} \sim 0.16$ T, while suppression of WAL occurs at $B'_{cr} \sim 1.1$ T.

4.2. *Strained* GaSb *whisker magnetoresistance*

Strain influences GaSb whisker magnetoresistance: longitudinal magnetoresistance jumps at low magnetic fields transits to negative magnetoresistance at increase of magnetic field intensity. As in the case of unstrained whiskers first magnetoresistance jump is probably connected with SC states. The second magnetoresistance jump at higher magnetic fields is interpreted as WAL, while negative magnetoresistance observed at further increasing magnetic field is called by WL of charge carriers. Let us consider the phenomena in detail.

An analysis of upper critical magnetic fields (see Fig. 4) gives zero temperature critical magnetic field 0.1 T for SC suppression. The corresponding results are provided on insert of Fig. 4. Therefore, strain leads to decrease of SC in the whiskers, which is observed from the decrease of its magnetic field suppression.

Taking into account the magnetic flow Φ_0, one can calculate the superconductive coherence length ξ

$$B_C = \Phi_0 / 2\pi\xi^2, \tag{1}$$

where Φ_0 is the flux quantum, we obtained superconductor coherence length $\xi = 5$ nm.

Analysis of the second jumps of longitudinal magnetoresistance at low magnetic fields and different temperatures allows us to obtain the upper critical field for breakdown of the spin orientation of charge carriers at their WAL. The resulting B'_{cr} is obvious on Fig. 5(a) and consists of 0.32 T.

The negative magnetoresistance observed at higher magnetic fields is likely connected with WL of charge carriers. One can analyze the field dependency of magnetoresistance. As for now, there are experimental results that proved the satisfaction of the Mott law in heavily doped semiconductors. It has been shown in [30] that the following expression is valid for two different temperatures: $H_0^1 / H_0^2 = (T_1 / T_2)^{1/2}$, where H_0 is the magnetic field, at which magnetoresistance is equal to zero. According to theoretical assumptions presented in [17], this magnetic field is proportional to the temperature of observation ($H_0 \sim T^{3/8}$) (insert of Fig. 3(b)), that has been evidenced

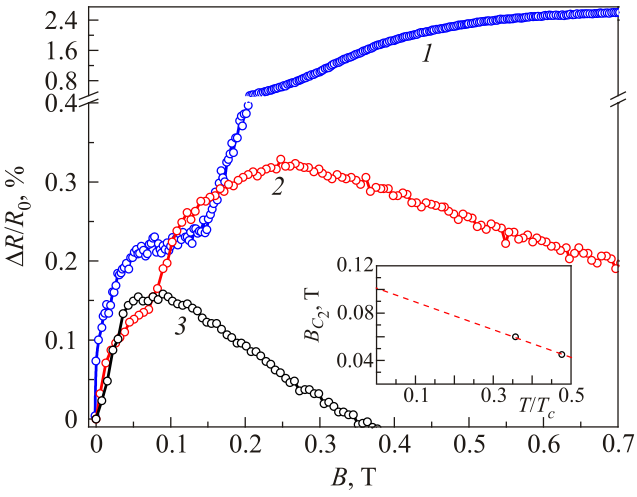

Fig. 4. (Color online) Longitudinal magnetoresistance of strained GaSb whiskers at temperature, K: 1.5 (*1*), 2 (*2*), 4.2 (*3*). Insert: zero temperature critical magnetic field.

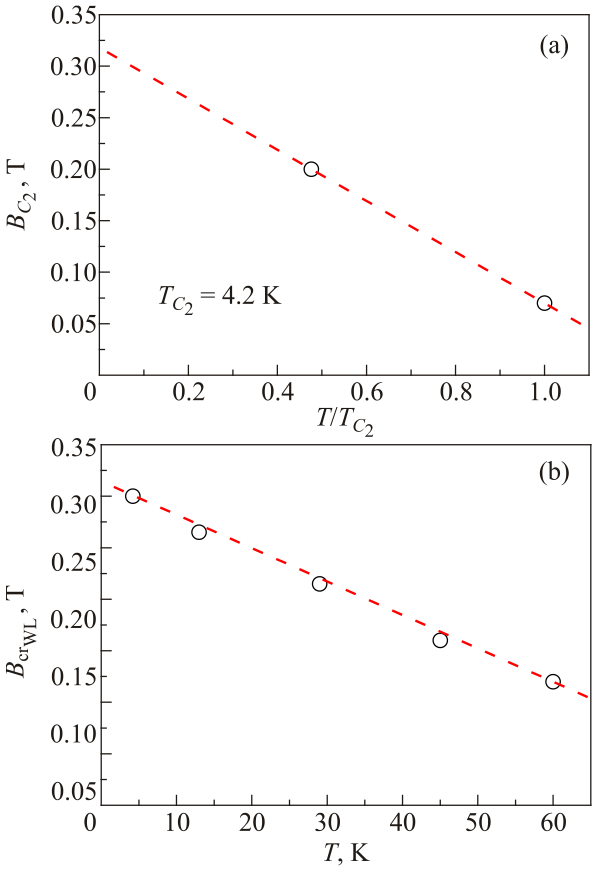

Fig. 5. Zero critical magnetic field in strained GaSb whiskers for SC (a) and WAL (b).

during the experimental studies. This fact confirms the Mott hopping conductivity at $B = 0$.

Thus, WL is connected with interaction of two carriers localized on one impurity with opposite spins. Magnetic field application leads to breakdown of spin ordering which is accompanied by substantial decrease of the whisker magnetoresistance. At certain magnetic field intensity a saturation of the effect occurs that is observed at Fig. 3(b) as minimum of magnetoresistance.

Let us consider temperature dependences of the whisker resistance. A comparison of curves *1* and *2* on $R(T)$ dependences for strained and unstrained samples indicates that strain leads to appearance of metal–insulator transition at temperature below 10 K (see Fig. 1(b)). One can obtain the energy activation of the hopping conductance, which was calculated from $\ln(1/R) = f(1/T)$ dependency and equal to 0.7 meV.

Taking into account the longitudinal magnetoresistance of strain GaSb whiskers (Fig. 3(b)) one can obtain the critical magnetic field for suppression of WL (see Fig. 5(b)). The value is equal to 0.31 T, which is similar with the critical magnetic field for breakdown of spins at WAL. Thus, the effects have the same critical magnetic field suppression.

To describe the nonmonotonic character of magnetoresistance of strained GaSb whiskers let us consider three-dimensional quantum subband electrons. Three electron subbands (the insert of Fig. 6) were under the consideration. The parabola (*1*) corresponded to the lowest states ($N_1 = N_2 = 0$), while parabola (*2*) represented first size quantized zone ($N_1 = 0$; $N_2 = 1$), parabola (*3*) was described by quantum numbers ($N_1 = 1$; $N_2 = 0$). Size quantized band (1) would be twice degenerated without the action of a magnetic field or strain. Taking into account the above subbands of the size quantized zone, one can explain peculiarities of magnetoresistance dependence in GaSb whiskers on application of the longitudinal magnetic field (Fig. 6(a)).

Let us consider three cases.

(a) A chemical potential level without the action of a magnetic field is greatly lower than the bottom of the subband that was twice degenerated in this case. At increase of magnetic field intensity the chemical potential ξ_0 decreases monotonously, which is accompanied with a rise of the whisker magnetoresistance (see Fig. 6(a), curve *1*).

(b) A chemical potential matches or is slightly below the bottom of the second subband. Then with increasing magnetic field B, the chemical potential decreases and the magnetoresistance initially decreases and then increases monotonically (Fig. 6(a), curve *2*).

(c) A chemical potential is slightly above the bottom of the second subband. Then with increasing magnetic field the magnetoresistance first increases and then, when ξ_0 passes the subband bottom, sharply enough falls. With the further increase in the magnetic field, it grows monotonously (Fig. 6(a), curve *3*).

The last case (Fig. 6(a), curve *3*) explains quite well the experimental dependence of the longitudinal magnetore-

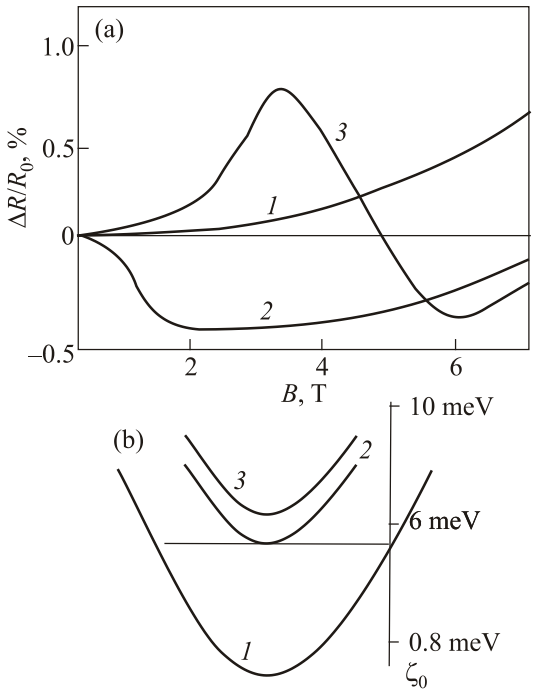

Fig. 6. (a) Theoretical dependences of reduced magnetoresistance in GaSb whiskers; (b) schematic representation of quantum subband with a position of chemical potential.

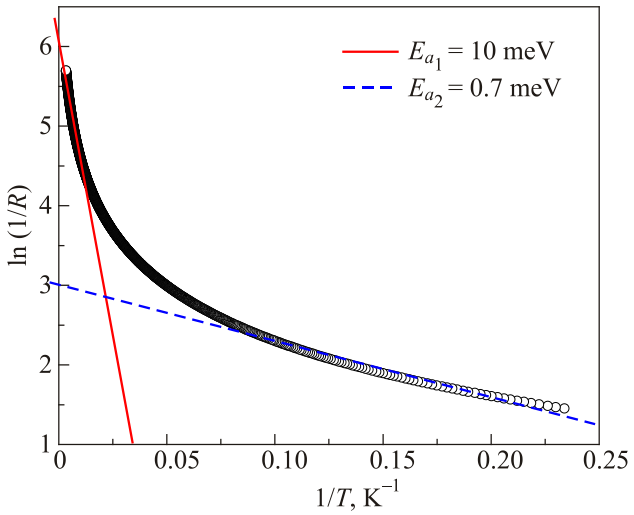

Fig. 7. (Color online) Activation energy of WAL 0.7 meV in the temperature range 4–10 K and 10 meV in the temperature range 50–100 K.

sistance of GaSb whiskers (see for example Fig. 3(b), curve *2*) in small magnetic fields at temperature 4.2 K. So, strained longitudinal magnetoresistance changes the sign and crosses from positive to negative at various magnetic fields. At further increase of temperature $T > 10$ K the longitudinal magnetoresistance for strained samples (Fig. 3(b), curves *3*, *4*) becomes negative in all range of the magnetic field according to theoretical data of Fig. 6, curve *2*. Therefore, thermal energy kT leads to transition of chemical potential below the bottom of the second subband. The case (b) corresponds also to field dependency of transverse magnetoresistance in the temperature range 4.2–60 K (Fig. 2(b)). As obvious from Fig. 2(b) at temperature higher than 60 K the whisker magnetoresistance corresponds to case (a), i.e., classical behavior of magnetoresistance. Thermal energy of the process corresponds to 6 meV. However, still unclear is the cause of size quantization of electrons in the whiskers rather large diameter (of the order of tens of microns).

The observed phenomenon could be explained in other way. Fundamentally, it should be noted that the prevalence of surface conductance in the specimens as compared with bulk one. Thus, the whisker growth by chemical vapor deposition in halogen closed system leads to the increase of dopant impurity approaching the whisker surface. There are various parameters that influence impurity distribution. For instance, gain in impurity doping near the whisker surface might be caused by diffusion of impurities to the surface during the sample annealing after growth.

Provided the assumption of the pervasiveness of surface conductance in the whisker is accurate, i.e., the main part of charge carriers transport takes place in the subsurface layers of the whisker, which can be characterized by effective wire radial distance dW, it can be concluded that the magnetoresistance peaks in Fig. 3 are present as a consequence of the classical size effect, where the wire boundary scattering is reduced as the cyclotron radius becomes smaller than the effective wire radial distance, resulting in a decrease in the resistivity. The same behavior is typical for the magnetoresistance of InSb whiskers, while the peak position B_m varies linearly with $1/dW$ as the wire diameter increases [21]. The possibility of B_m occurring is determined by $B_m \approx 2ck_F/EdW$, where k_F is the wavevector at the Fermi energy. Effective wire radial distance can be calculated taking into account obtained Fermi energy E that for GaSb whiskers ranges within $dW \sim 150$ nm.

Activation energy of WAL could be estimated taking into account a WAL temperature disappearing at 10 K (see Fig. 3(b), curve *3*). The estimated value of activation energy is about 0.8 meV. The value is in good agreement with the above activation energy obtained from $R(T)$ dependency 0.7 meV. Thus, strain leads to splitting of degenerate level on two components with opposite spins (WAL) and parallel spins (WL). Breakdown of WL occurs at temperatures higher than 60 K, which needs the activation energy of about 6 meV. On the other hand, activation energy determined from $\ln(1/R) = f(1/T)$ dependence in the temperature range 50–100 K consists of 10 meV (Fig. 7) that is in good accordance the value determined from the magnetoresistance data.

4. Conclusions

Strain influence on *n*-type conductivity GaSb whisker was studied at weak magnetic fields 0–3 T and low temperatures 1.5–60 K. Large minimum revealed on the temperature dependences of resistance at temperature below 11 K corresponds to the strain inducted metal–insulator transition to insulator phase. On the other hand, straight drop of the resistance at temperature about 4.2 K connected with the transition to the superconductive state.

The magnetic field can suppress SC and WAL effects for unstrained samples in the temperature range 1.5–4.2 K that allows us to found the upper critical zero magnetic fields, which consists 0.16 and 1.1 T, respectively. Strain influence on *n*-type conductivity GaSb whisker leads to suppression of SC and WL effects. The critical magnetic fields for SC and WL effects coincide and consist of about 0.31 T. Strain also induces splitting of degenerate level on two components with opposite and parallel spins connected with WAL and WL effects, respectively. The activation energy of WAL is equal to 0.7 meV, while it consists of 6 meV in the case of WL effect.

1. M.Z. Hasan and C.L. Kane, *Rev. Mod. Phys.* **82**, 3045 (2010).
2. X.-L.Qi and S.-C. Zhang, *Rev. Mod. Phys.* **83**, 1057 (2011).
3. H. Peng, K. Lai, D. Kong, S. Meister, Y. Chen, X.L. Qi, S.C. Zhang, Z.X. Shen, and Y. Cui, *Nat. Mater.* **9**, 225 (2010).
4. H. Steinberg, D. Gardner, Y. Lee, and P. Jarillo-Herrero, *Nano Lett.* **10**, 5032 (2010).
5. M.L. Tian, W. Ning, Z. Qu, H. Du, J. Wang, and Y. Zhang, *Sci. Rep.* **3**, 1212 (2013).

6. Y. Yan, Z.-M. Liao, Y.-B. Zhou, H.-Ch. Wu, Y.-Q. Bie, J.-J. Chen, J. Meng, X.-S. Wu, and D.-P. Yu, *Sci. Rep.* **3**, 1264 (2013).
7. Y. Wang, F. Xiu, L. Cheng, L. He, M. Lang, J. Tang, X. Kou, X. Yu, X. Jiang, Z. Chen, J. Zou, and K.L. Wang, *Nano Lett.* **12**, 1170 (2012).
8. J. Chen, H.J. Qin, F. Yang, J. Liu, T. Guan, F.M. Qu, G.H. Zhang, J.R. Shi, X.C. Xie, C.L. Yang, K.H. Wu, Y.Q. Li, and L. Lu, *Phys. Rev. Lett.* **105**, 176602 (2010).
9. H.-T. He, G. Wang, T. Zhang, I.-K. Sou, G.K.L. Wong, J.-N. Wang, H.-Z. Lu, S.-Q. Shen, and F.-C. Zhang, *Phys. Rev. Lett.* **106**, 166805 (2011).
10. H. Wang, H. Liu, C.-Z. Chang, H. Zuo, Y. Zhao, Y. Sun, Z. Xia, K. He, X. Ma, X.C. Xie, Q.-K. Xue, and J. Wang, *Sci. Rep.* **4**, 5817 (2014).
11. H.-Z. Lu and Sh.-Q. Shen, *Proc. of SPIE* **9167**, 91672E (2014).
12. J.G. Checkelsky, Y.S. Hor, R.J. Cava, and N.P. Ong, *Phys. Rev. Lett.* **106**, 196801 (2011).
13. H.T. He, G. Wang, T. Zhang, I.K. Sou, G.K. Wong, J.N. Wang, H.-Z. Lu, S.-Q. Shen, and F.-C. Zhang, *Phys. Rev. Lett.* **106**, 166805 (2011).
14. H. Steinberg, J.B. Laloe, V. Fatemi, J. Moodera, and P. Jarillo-Herrero, *Phys. Rev. B* **84**, 233101 (2011).
15. J.E. Moore, *Nature* **464**, 194 (2010).
16. J. Chen, D. Donetsky, L. Shterengas, M.V. Kisin, G. Kipshidze, and G. Belenky, *IEEE J. Quantum Electronics* **44** (12) (2008).
17. Y.-W. Chen, Z. Tan, L.-F. Zhao, J. Wang, Y.-Z. Liu, C. Si, F. Yuan, W.-H. Duan, and J. Xu, *Chinese Phys. B* **25**, 038504 (2016).
18. Y. Sun, S. Thompson, and T. Nishida, *J. Appl. Phys.* **101**, 104503 (2007).
19. F. Herling, C. Morrison, C.S. Knox, S. Zhang, O. Newell, M. Myronov, E.H. Linfield, and C.H. Marrows, *Phys. Rev. B* **95**, 155307 (2017).
20. A.A. Druzhinin, I.I. Maryamova, and O.P. Kutrakov, *Funct. Mater.* **23**, 206 (2016).
21. A.A. Druzhinin, I. Ostrovskii, Yu. Khoverko, and N. Liakh-Kaguy, *Fiz. Nizk. Temp.* **42**, 581 (2016) [*Low Temp. Phys.* **42**, 453 (2016)].
22. I. Khytruk, A. Druzhinin, I. Ostrovskii, Yu. Khoverko, N. Liakh-Kaguy, and K. Rogacki, *Nanoscale Research Lett.* **12**, 156 (2017).
23. A. Druzhinin, I. Ostrovskii, Y. Khoverko, K. Rogacki, and N. Liakh-Kaguy, *Appl. Nanosci.* **8**, 877 (2018).
24. A.A. Druzhinin, N.S. Liakh-Kaguy, I.P. Ostrovskii, Yu.M. Khoverko, and K. Rogacki, *J. Nano- and Electronic Phys.* **9**(5), 05013 (2017).
25. A. Druzhinin, I. Ostrovskii, Yu. Khoverko, and N. Liakh-Kaguy, *Fiz. Nizk. Temp.* **43**, 871 (2017) [*Low Temp. Phys.* **43**, 692 (2017)].
26. A. Druzhinin, I. Ostrovskii, Yu. Khoverko, N. Liakh-Kaguy, and K. Rogacki, *Fiz. Nizk. Temp.* **44**, 1521 (2018) [*Low Temp. Phys.* **44**, 1189 (2018)].
27. V.V. Andrievskiĭ, I.B. Berkutov, Yu.F. Komnik, O.A. Mironov, and T.E. Whall, *Fiz. Nizk. Temp.* **26**, 1202 (2000) [*Low Temp. Phys.* **26**, 890 (2000)].
28. I.B. Berkutov, Yu.F. Komnik, V.V. Andrievskii, O.A. Mironov, M. Myronov, and D.R. Leadley, *Fiz. Nizk. Temp.* **32**, 896 (2006) [*Low Temp. Phys.* **32**, 683 (2006)].
29. D.R. Leadley, V.V. Andrievskii, I.B. Berkutov, Y.F. Komnik, T. Hackbarth, and O.A. Mironov, *J. Low Temp. Phys.* **159**, 230 (2010).
30. R.F. Konopleva, *Galvanomagnetic properties of disordered semiconductors*, Moscow Publishing House, Moscow (1980), p. 25 (in Russian).

Надпровідність та слабка антилокалізація у ниткоподібних кристалах GaSb під впливом деформації

Н. Лях-Кагуй, А. Дружинін, І. Островський, Ю. Ховерко

Досліджено вплив деформації на поведінку температурних залежностей опору в ниткоподібних кристалах GaSb *n*-типу провідності з концентрацією телуру $1{,}7\cdot10^{18}$ см$^{-3}$. На основі аналізу цих залежностей в інтервалі температур 4,2–30 К виявлено індукований деформацією перехід метал–діелектрик, а також перехід у надпровідний стан. Для недеформованих і деформованих ниткоподібних кристалів GaSb також вивчено поперечний та поздовжній магнітоопір в інтервалі магнітних полів 0–3 Тл та температур 1,5–60 К, у яких спостерігались такі ефекти, як надпровідність і слабка антилокалізація. Визначено значення верхнього критичного магнітного поля придушення надпровідності в зразках GaSb, а також виявлено послаблення ефекту надпровідності внаслідок деформації. Встановлено, що в ниткоподібних кристалах GaSb *n*-типу провідності деформація зумовлює розщеплення виродженого рівня на дві компоненти з паралельними і протилежними спінам, яке спричинене ефектами слабкої локалізації та антилокалізації відповідно.

Ключові слова: ниткоподібні кристали GaSb, вплив деформації, поперечний та поздовжній магнітоопір, надпровідність, слабка локалізація та антилокалізація.

Сверхпроводимость и слабая антилокализация в нитевидных кристаллах GaSb под влиянием деформации

Н. Лях-Кагуй, А. Дружинин, И. Островский, Ю. Ховерко

Исследовано влияние деформации на характер температурных зависимостей сопротивления в нитевидных кристаллах GaSb *n*-типа проводимости с концентрацией теллура $1{,}7\cdot10^{18}$ см$^{-3}$. На основе анализа этих зависимостей в диапазоне температур 4,2–30 К обнаружены индуцированный деформацией переход металл–диэлектрик, а также переход в сверхпроводящее состояние. Для недеформированных и де-

формированных нитевидных кристаллов GaSb также исследованы поперечное и продольное магнитосопротивление в интервале магнитных полей 0–3 Тл и температур 1,5–60 К, в которых наблюдались такие эффекты, как сверхпроводимость и слабая антилокализация. Определено значение верхнего критического магнитного поля подавления сверхпроводимости в образцах GaSb, а также установлено ослабление эффекта сверхпроводимости под действием деформации. Обнаружено, что в нитевидных кристаллах GaSb *n*-типа проводимости деформация приводит к расщеплению вырожденного уровня на две компоненты с параллельными и противоположными спинами, которое вызвано эффектами слабой локализации и антилокализации соответственно.

Ключевые слова: нитевидные кристаллы GaSb, влияние деформации, поперечное и продольное магнитосопротивление, сверхпроводимость, слабая локализация и антилокализация.